Full Paper

Urantide Conformation and Interaction with the Urotensin-II Receptor

Diego Brancaccio[1]*, Antonio Limatola[1]*, Pietro Campiglia[2], Isabel Gomez-Monterrey[1], Ettore Novellino[1], Paolo Grieco[1], and Alfonso Carotenuto[1]

[1] Department of Pharmacy, University of Naples "Federico II", Naples, Italy
[2] Department of Pharmacy, University of Salerno, Fisciano, Salerno, Italy

Urotensin II (U-II) is a disulfide bridged peptide hormone identified as the ligand of a G protein-coupled receptor. Human U-II (H-Glu-Thr-Pro-Asp-c[Cys-Phe-Trp-Lys-Tyr-Cys]-Val-OH) has been described as the most potent vasoconstrictor compound identified to date. We have previously identified the compound termed urantide (H-Asp-c[Pen-Phe-DTrp-Orn-Tyr-Cys]-Val-OH), which is the most potent UT receptor (UTR) antagonist described to date. Urantide may have potential clinical value in the treatment of atherosclerosis. In the present study, we studied the conformational preferences of urantide in DPC micelles and developed a urantide/UTR interaction model. This model can help the design of novel peptides and small molecules as UTR antagonists.

Keywords: Atherosclerosis / Conformation by NMR / Docking studies / Therapeutic peptide / Urotensin-II

Received: July 19, 2013; Revised: September 17, 2013; Accepted: September 23, 2013

DOI 10.1002/ardp.201300269

Additional supporting information may be found in the online version of this article at the publisher's web-site.

Introduction

Urotensin-II (U-II) belongs to a series of regulatory neuropeptides first isolated from the urophysis of the teleost fish *Gillichthys mirabilis* [1]. It was subsequently found in tetrapods [2] and its precursor cloned in various vertebrate species including frog, rat and mouse, pig, monkey, and human [3–6]. U-II actions are mediated by a specific cell surface G protein-coupled receptor [7], named UT receptor (UTR).

Recently, an analog of U-II, called urotensin-related peptide (URP), has been identified in mammals [8]. In all U-II and URP isoforms known so far, the sequence of the cyclic C-terminal hexapeptide has been fully conserved across species [9]. The U-II and URP genes are primarily expressed in motoneurons located in discrete brainstem nuclei and in the ventral horn of the spinal cord [10–13]. U-II and URP mRNAs have also been detected, at a much lower level, in various peripheral tissues including the pituitary gland, heart, spleen, thymus, pancreas, kidney, small intestine, adrenal gland, and prostate [3, 8, 14].

The U-II/UT receptor system plays an important role in cardiovascular functions; in fact, hU-II, human urotensin-II peptide (hU-II) has been shown to be 1–2 orders of magnitude more potent than endothelin-1 in producing vasoconstriction in mammals and thus is one of the most effective vasoconstrictor compounds identified to date [7, 15, 16]. Based on its spectrum of activities, hU-II emerges as a modulator of the cardiovascular homeostasis, and therefore may be involved in certain cardiovascular pathologies [15–17]. It has been recently demonstrated that U-II is involved in inhibition of insulin release [18] in the perfused rat pancreas, may play an important role in pulmonary hypertension [19], and modulates erectile function through eNOS [20]. Central nervous effects of U-II have also been described [21]. Hence, the hU-II antagonists could be of therapeutic value in a number of pathological disorders [22, 23]. Increasing interest in the identification of U-II/UTR system modulators as

Correspondence: Alfonso Carotenuto, Dipartimento di Farmacia, Università di Napoli "Federico II", Via D. Montesano, 49, 80131 Napoli, Italy.
E-mail: alfonso.carotenuto@unina.it
Fax: +39 081 678630

*These two authors contributed equally to this work.

potential drugs prompted the development of low-molecular-weight compounds as nonpeptide UT receptor agonists and antagonists [24]. The optimization of a peptide as a lead structure is important to improve its pharmacokinetic properties and in identifying the pharmacophore elements, that is, to determine the key amino acid residues that are involved in the biological activity [25]. It has been previously demonstrated that the C-terminal octapeptide of U-II retains full biological activity and binding properties [26–32]. Interestingly, some common features (two aryl moieties and a protonable nitrogen atom) are observable in peptide and non-peptide UTR ligands [33]. Hence, the structural information obtained by the peptide investigation might be useful for the design of both small molecules and peptide ligands. Our research group has been involved for a long time in the development of UTR peptide ligands [34]. We have identified both a superagonist named P5U (H-Asp-c[Pen-Phe-Trp-Lys-Tyr-Cys]-Val-OH) [35] and an antagonist urantide (H-Asp-c[Pen-Phe-DTrp-Orn-Tyr-Cys]-Val-OH) [36] of hU-II (Table 1). Urantide antagonistic effect is 50 times stronger than that of other chemical compounds [37]. Interestingly, it has been recently found that urantide protects against atherosclerosis in rats [38]. Previously, we performed extensive nuclear magnetic resonance (NMR) and computational studies on both P5U and urantide that allowed us to formulate a hypothesis about the structural changes that determine the switching from agonist to antagonist activity [39–41]. Recently, using P5U and urantide conformationally constrained analogs, we gained new insight into the putative active conformation of ligands at UTR [42]. In this work, we determined the solution conformation of urantide using dodecylphosphocholine (DPC) as membrane mimetic environment and docked the obtained structure of urantide within a theoretical model of UTR. Differences between this model and that previously reported are discussed. The new model can help the design of novel peptides and small molecules as antagonists at the UTR.

Table 1. Sequence, receptor affinity[a)], and biological activity[a)] of P5U and urantide.

H-Asp-c[Pen-Phe-***Xaa-Yaa***-Tyr-Cys]-Val-OH					
Peptide	**Xaa**	**Yaa**	**pK_i[b)]**	**pEC_{50}[c)]**	**pK_B[d)]**
P5U	Trp	Lys	9.70 ± 0.07	9.60 ± 0.07	–
Urantide	DTrp	Orn	8.30 ± 0.04	Inactive	8.30

[a)] Values reported in [42].
[b)] pK_i: $-\log K_i$ affinity values are from [^{125}I]urotensin II binding inhibition experiments at the human urotensin receptor.
[c)] pEC_{50}: $-\log EC_{50}$.
[d)] pK_B ($-\log K_B$) values are from experiments in the rat thoracic aorta.

Results

NMR analysis

A whole set of 1D and 2D NMR spectra in 200 mM aqueous solution of DPC were collected for urantide. Complete ^{1}H NMR chemical shift assignments were effectively achieved for the peptide according to the Wüthrich procedure [43] via the usual systematic application of double quantum filtered correlated spectroscopy (DQF-COSY) [44, 45], total correlated spectroscopy (TOCSY) [46], and nuclear Overhauser enhancement spectroscopy (NOESY) [47] experiments with the support of the XEASY software package (Supporting Information Table S2) [48].

A qualitative analysis of short- and medium-range nuclear Overhauser effects (NOEs), $^3J_{NH\text{-}H\alpha}$ coupling constants, NH exchange rates, and temperature coefficients for exchanging NH indicated that urantide shows stable secondary structure in DPC micelles (Supporting Information Table S2). In particular, NOE contacts between H_α-NH_{i+2} of D-Trp^7 and Tyr^9 and between NH–NH_{i+1} of Orn^8 and Tyr^9 indicated the presence of a β-turn. This result was supported by the observation of slowly exchanging NH resonance of residue 9, and low value of the temperature coefficient for this proton ($-\Delta\delta/\Delta T < 3.0$ ppb/K). A short stretch of antiparallel β-sheet involving residues 5–6 and 10–11 is inferred from a number of long-range NOEs including H_α-NH connectivities between residues 5, 11 and 10, 6 and a NH–NH connectivity between residues 6 and 9. All the data indicated the presence of a β-hairpin structure. Considering the side chain orientations, urantide shows interchain NOEs between residues D-Trp^7 and Orn^8, and between Phe^6 and Val^{11}. Furthermore, Tyr^9 aromatic proton signals show NOE contacts with both Orn^8 and Val^{11} side chains. The last interaction was relatively strong, indicating that the conformer bearing a close contact between Tyr^9 and Val^{11} side chains is highly populated.

NOE-derived constraints obtained for urantide (Supporting Information Table S3) were used as the input data for a simulated annealing structure calculation. Ten calculated structures satisfying the NMR-derived constraints (violations smaller than 0.40 Å) were chosen for further analysis (Fig. 1). Urantide shows a type II′ β-hairpin structure encompassing residues 5–10 (backbone rmsd value is 0.17 Å). Considering the side chains orientation, D-Trp^7 and Lys^8 side chains showed a large preference for *trans* and g^- rotamer, respectively. The χ_2 dihedral angle of D-Trp^7 was 125° or −70° ($\chi_2 = -67°$ in the lowest energy conformation) in accordance with strong NOEs between H^α and $H^{\varepsilon 3}$ or $H^{\delta 1}$, respectively (Supporting Information Table S3). Finally, Tyr^9 is found both in *trans* and g^- conformations, with a prevalence of the *trans* rotamer. Therefore, D-Trp^7 indole is close to Lys^8, and Tyr^9 phenolic ring points toward Val^{11}. Obtained

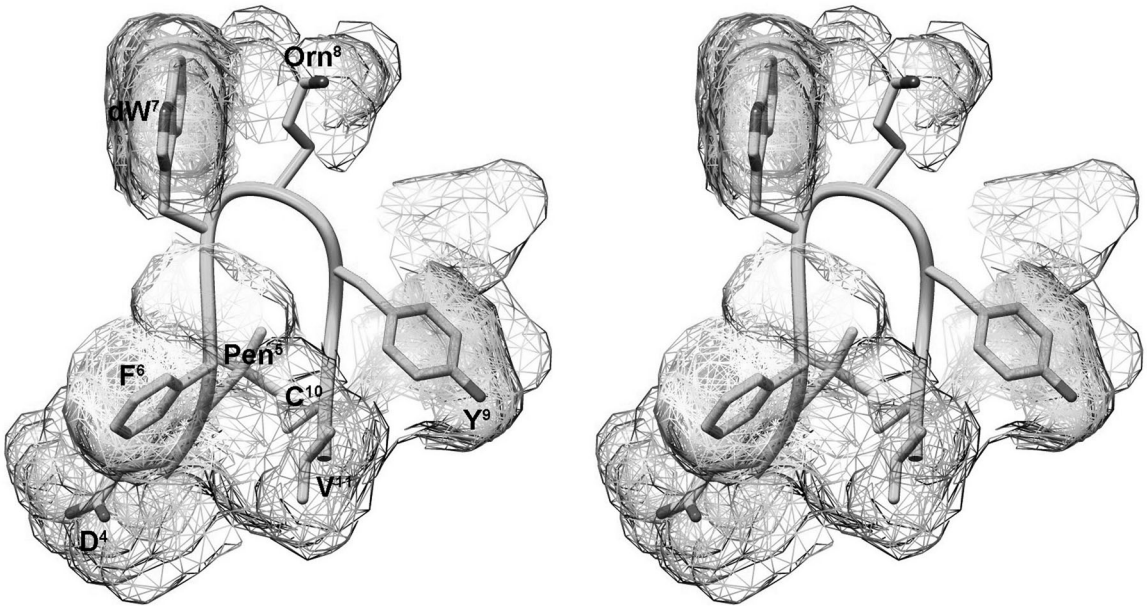

Figure 1. Stereoview of the lowest-energy conformer of urantide. Backbone is evidenced as a ribbon. Side chains of the 10 lowest-energy conformers are also shown as mesh surface.

conformations are in accordance with the measured $^{3}J_{HN-H\alpha}$ and $^{3}J_{H\alpha-H\beta}$ coupling constants (Supporting Information Table S2).

Docking studies

The theoretical structure of the h-UT receptor was generated by homology modeling based on the crystal structure of bovine rhodopsin (PDB code 1F88) [49], as described previously [41]. The resulting structure represents an inactive form of the h-UT receptor with an overall conformation very similar to that of bovine rhodopsin (1.22 Å rmsd between the backbone atoms of the transmembrane domains) and to the β_2-adrenergic receptor (β_2AR, PDB code 2RH1) [50]. Calculations converged toward a single solution in which the lowest-energy binding conformation also belonged to the most populated cluster and was remarkably stable throughout the molecular dynamic (MD) simulations (pdb coordinates are available on email request). As shown in Fig. 2a, the hypothetical binding site of urantide is located among TM-III/TM-VII, EL-II, and EL-III. The β-hairpin is oriented along the receptor helical axis, with the N- and C-terminal residues pointing toward the extracellular side. The binding mode of the peptide is determined mainly by the interactions shown in Fig. 2b and Table 2. In particular, (i) a tight charge-reinforced hydrogen-bonding network involving the carboxylate group of Asp130 and the protonated δ-amino group of Orn^8 of urantide is established. (ii) Two hydrophobic pockets, delimited by residues listed in Table 2, host the aromatic side chains of Phe^6 and D-Trp^7, of urantide. Particularly, the indole system of D-Trp^7 appears to be optimally oriented for a π-stacking interaction with the aromatic indole system of Trp275. (iii) The phenolic OH of Tyr^9 is at hydrogen-bonding distance with the backbone CO of Ala289. (iv) Asp^4 in urantide is involved in a hydrogen-bonding network. (v) Finally, the negatively charged C-terminal group establishes two hydrogen bonds with backbone HN of Cys123 and Cys 199, and a salt bridge with the protonated guanidinium moiety of Arg189. All the aforementioned interactions resulted to be quite stable during the whole MD production run (data not shown).

Discussion

In our previous studies, we showed that all hU-II analogs, which retain high affinity for UT receptor, possess a type II′ β-hairpin backbone conformation regardless of their agonist or antagonist activity, indicating that such backbone conformation is necessary for the UT recognition [39, 40]. We hypothesized that the main conformational difference observed in the structures of the antagonists and the agonists was a different orientation of the (D/L)-Trp^7 side chain. This hypothesis has been challenged by recent results about the activity of P5U and urantide analogs in which the Trp^9 was replaced by the highly constrained analog Tpi [42]. Tpi (2,3,4,9-tetrahydro-1*H*-pyrido[3,4-*b*]indole-3-carboxylic acid) can only possess gauche side chain rotamer populations since the indole moiety is cyclized to the peptide backbone N$^{\alpha}$ [51].

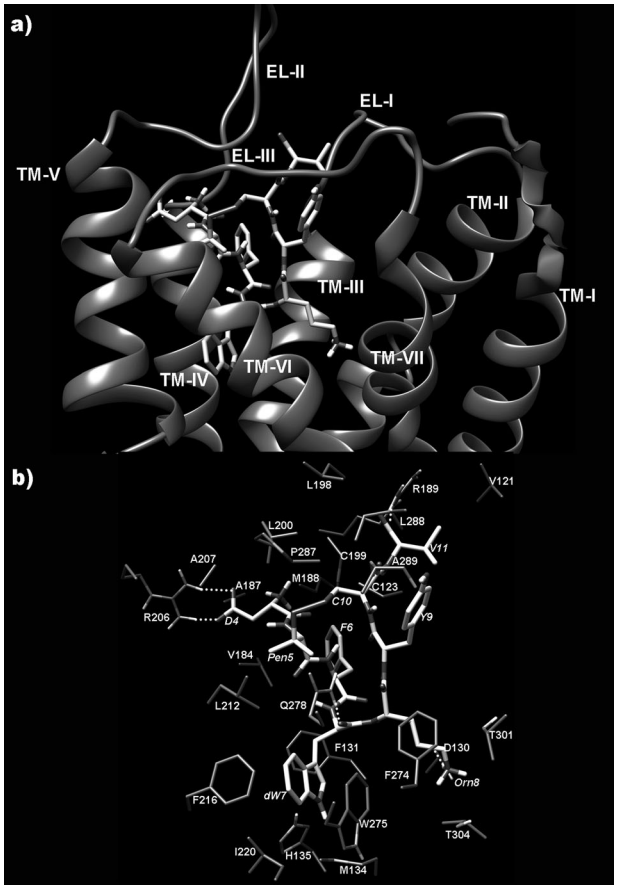

Figure 2. (a) h-UTR model complexed with urantide. Receptor backbones are represented in gray and labeled. (b) Urantide within the binding pocket of h-UTR. Hydrogen bonds are shown as dotted lines.

Nevertheless, we found derivatives showing both agonist and antagonist activity only depending on the presence of Lys (agonist) or Orn (antagonist) at position 8. Conformational analysis indicated that the main difference between agonist and antagonist 3D structure was the orientation of the Tyr^9 side chain, which was gauche$^-$ oriented in the agonist P5U and *trans* oriented in the antagonist urantide. Consequently, phenol ring is close to Lys^8 or far from Orn^8, respectively. Tyr^9 side chain orientation is mainly defined by NOEs with Lys^8/Orn^8 or Val^{11} side chain signals. In our previous conformational study on the lead antagonist urantide [40], we found a gauche$^-$ orientation for Tyr^9 side chain but the above-mentioned NOE could not be observed in its NOESY spectrum due to signal overlapping. In the cited work [41], NMR study was performed in sodium dodecylsulfate (SDS) micelle solution, which is largely used for the conformation analysis of peptide hormones [52–54]. Here trying to avoid the overlapping problems, we repeated the conformational analysis of urantide using another micelle solution, i.e., DPC. Also, DPC solutions are commonly used for peptide hormones [55, 56] and antimicrobial peptides [57, 58] studies. NMR data obtained using a DPC solution are very similar to those obtained in SDS solution, but luckily signals show a better dispersion. In particular, for urantide the NOEs between Orn^8 and Val^{11} side chains are clearly visible. Urantide structure obtained from these NOEs (Fig. 1) showed Tyr^9 both in *trans* and in g$^-$ conformations, with a prevalence of the *trans* rotamer. Therefore, Tyr^9 phenolic ring is close to Val^{11} in urantide accordingly to the results recently found for constrained analogs [42]. Furthermore, D-Trp^7 side chain is stably in *trans* conformation as derived by the strong NOEs between its indole moiety and the Orn8 side chain. This was more flexible in the urantide structure obtained in SDS. Again, signal overlapping in the NOESY spectrum acquired in the last medium can explain the observed differences.

To gain insight into the interaction mode, the new structure of urantide was docked within a model of human urotensin II (receptor h-UTR) that we recently built [41]. The binding mode of the peptide is determined mainly by the interactions shown in Fig. 2b and Table 2 and described in the Results section. The main difference, compared to the previously obtained model complex [41], is observed in the interactions of the Tyr^9 side chain, as expected from the starting NMR ligand structure. A superposition of the

Table 2. Urantide/h-UTR interactions.

Residue[a)]	Surrounding residue
Asp^4	Ala187 (EL-II), Met188 (EL-II), Cys199 (EL-II), Arg206 (EL-II), Ala207 (EL-II)
Pen^5	Leu200 (EL-II), Ala207 (EL-II), Leu212 (TM-V), Gln278 (TM-VI)
Phe^6	Cys123 (EL-I), Val184 (TM-IV), Met188 (EL-II), Cys199 (EL-II)
D-Trp^7	Phe131 (TM-III), Met134 (TM-III), His135 (TM-III), Leu212 (TM-V), Phe216 (TM-V), Ile220 (TM-V), Trp275 (TM-VI), Gln278 (TM-VI)
Orn^8	Asp130 (TM-III), Phe274 (TM-VI), Gln278 (TM-VI), Thr301 (TM-VII), Thr304 (TM-VII)
Tyr^9	Leu288 (EL-III), Ala289 (EL-III)
Cys^{10}	Cys199 (EL-II), Pro287 (EL-III), Leu288 (EL-III).
Val^{11}	Val121(EL-I), Cys123 (EL-I), Arg189 (EL-II), Leu198 (EL-II), Cys199 (EL-II), Leu288 (EL-III)

[a)] For the sake of clarity, the residue numbers of the ligands are reported as apex while those of the receptor are not.

two models is shown in Fig. S1 of the Supporting Information. Tyr[9] side chain points toward the third extracellular loops and forms a stable hydrogen bond with the backbone carbonyl of Ala289. In contrast, Tyr[9] side chain pointed toward the intracellular side of the receptor in the old model. An intriguing difference is that the Tyr[9] side chain is now highly exposed to the solvent while before it was hidden in a hydrophobic pocket. Interestingly, the urantide/UTR complex model described here shows comparable energy to the previously obtained one (Table 3) but it is in higher accordance with the current experimental data.

Based on the binding mode of UTR/urantide, we derived a new 3D pharmacophore model for peptide antagonists illustrated in Fig. 3. Distances between Tyr phenol moiety and Trp indole or Orn N^{δ} are longer than those reported previously for urantide in SDS solution [41] but are in good accordance with those recently reported for a highly constrained analog of the same peptide [42].

Conclusions

In conclusion, we determined the solution conformation of urantide using DPC as membrane mimetic environment and obtained a complex model of urantide within a theoretical model of UTR. A new three-point pharmacophore model has also been developed. Complex and pharmacophore models can help the next design cycle of novel peptide and small-molecule antagonists at UTR with potential anti-atherosclerotic activity.

Experimental

Peptide synthesis

Urantide was synthesized as previously described [36]. Analytical RP-HPLC indicated a purity >98%, and molecular weight was confirmed by ESI-MS analyses performed by API 2000 (Supporting Information, Table S1).

Table 3. Binding free energies (ΔG_{AD4}) calculated for the energy minimized averaged complexes deriving from the MD simulations.

Receptor	Ligand	ΔG_{bind}[a)]	Electr[b)]	H-bond[b)]	VdW[b)]	Desolv[b)]	Tors[b)]
h-UTR	Urantide	−22.74	−4.94	−5.35	−25.91	7.49	5.97
h-UTR[c)]	Urantide	−24.33	−4.99	−5.90	−26.50	7.09	5.97

[a)] ΔG_{bind}: free energy of binding.
[b)] Energy terms contributing to the AutoDock4 scoring function. Electr, electrostatic; H-bond, H-bonding; VdW, Van der Waals; Desolv, desolvation; Tors, torsional entropy. All terms are given in kcal/mol.
[c)] Previously reported model, [39].

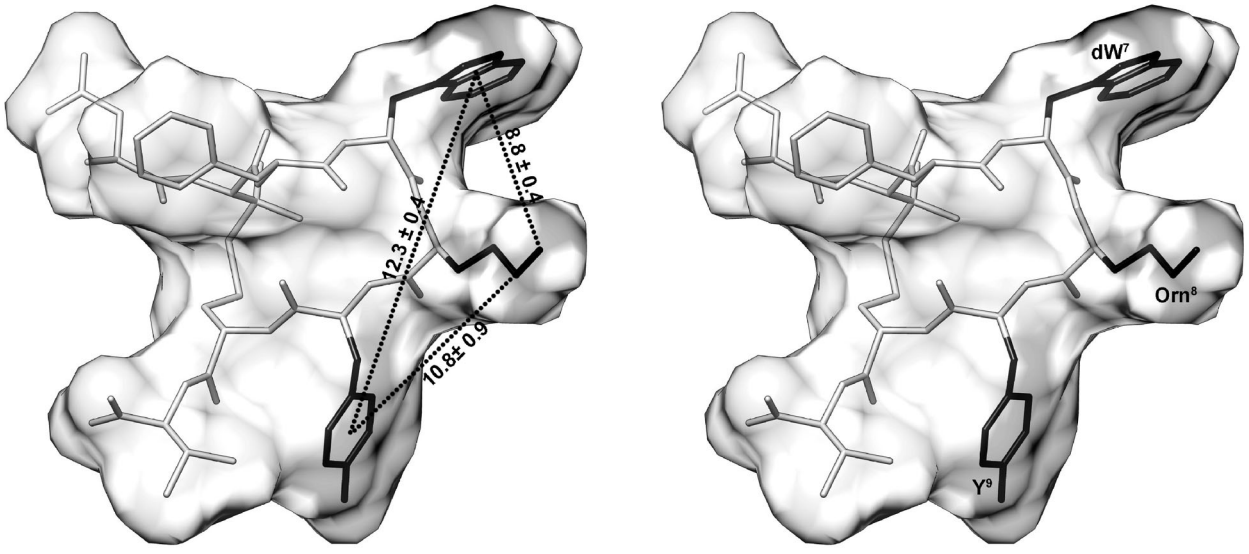

Figure 3. Stereoview of the pharmacophore model for peptide antagonists at UTR. The distances between the aryl ring centroids of (D)Trp[7] and Tyr[9], and the N^{δ} of Orn[8], are displayed. Distances and standard deviations are obtained from 100 structures saved every 10 ps of the MD simulations.

NMR sample preparation

99.9% ^2H_2O was obtained from Aldrich (Milwaukee, USA), 98% DPC-d_{38} was obtained from Cambridge Isotope Laboratories, Inc. (Andover, USA), and [(2,2,3,3-tetradeuterio-3-(trimethylsilanyl)]propionic acid (TSP) was obtained from MSD Isotopes (Montreal, Canada).

NMR spectroscopy

The samples for NMR spectroscopy were prepared by dissolving the appropriate amount of urantide in 0.45 mL of ^1H_2O (pH 5.5), 0.05 mL of ^2H_2O to obtain a concentration of 2 mM of peptide and 200 mM of DPC-d_{38}. NH exchange studies were performed dissolving peptide in 0.50 mL of ^2H_2O and 200 mM of DPC-d_{38}. NMR spectra were recorded on a Varian INOVA 700 MHz spectrometer equipped with a z-gradient 5 mm triple-resonance probe head. All the spectra were recorded at a temperature of 25°C. The spectra were calibrated relative to TSP (0.00 ppm) as internal standard. One-dimensional (1D) NMR spectra were recorded in the Fourier mode with quadrature detection. The water signal was suppressed by gradient echo [59]. 2D DQF-COSY [44, 45], TOCSY [46], and NOESY [47] spectra were recorded in the phase-sensitive mode using the method from States et al. [60]. Data block sizes were 2048 addresses in t_2 and 512 equidistant t_1 values. Before Fourier transformation, the time domain data matrices were multiplied by shifted $\sin^2$ functions in both dimensions. A mixing time of 70 ms was used for the TOCSY experiments. NOESY experiments were run with mixing times in the range of 50–200 ms. The qualitative and quantitative analyses of DQF-COSY, TOCSY, and NOESY spectra were obtained using the interactive program package XEASY [48]. $^3J_{HN\text{-}H\alpha}$ and $^3J_{H\alpha\text{-}H\beta}$ coupling constants were obtained from 1D ^1H NMR and 2D DQF-COSY spectra. The temperature coefficients of the amide proton chemical shifts were calculated from 1D ^1H NMR and 2D TOCSY experiments performed at different temperatures in the range 25–40°C by means of linear regression.

Structural determinations

The NOE-based distance restraints were obtained from NOESY spectra collected with a mixing time of 100 ms. The NOE cross peaks were integrated with the XEASY program and converted into upper distance bounds using the CALIBA program incorporated into the program package DYANA [61]. Cross peaks, which were overlapped more than 50%, were treated as weak restraints in the DYANA calculation. Only NOE-derived constraints were considered in the annealing procedures. An ensemble of 200 structures was generated with the simulated annealing of the program DYANA. An error-tolerant target function (tf-type = 3) was used to account for the peptide intrinsic flexibility. Non-standard Pen and Orn residues were added to DYANA residue library using MOLMOL [62]. From the produced 200 conformations, 50 structures were chosen, whose interprotonic distances best fitted NOE-derived distances, and then refined through successive steps of restrained and unrestrained energy minimization (EM) using the Discover algorithm (Accelrys, San Diego, CA) and the consistent valence force field (CVFF) [63] as previously described [39]. The final structures were analyzed using the InsightII program (Accelrys). RMS deviation analysis between energy minimized structures was carried out with the program MOLMOL.

Docking procedures

The new version of the docking program AutoDock4 (AD4) [64], as implemented through the graphical user interface called AutoDockTools (ADT), was used for rigid docking of the urantide NMR lowest-energy structure and a theoretical structure of the h-UT receptor recently described [41].

Urantide and the receptor structure were converted to AD4 format files using ADT generating automatically all other atom values. The docking area was centered around the putative binding site. A set of grids of 60 Å × 60 Å × 60 Å with 0.375 Å spacing was calculated around the docking area for the ligand atom types using AutoGrid4. For each ligand, 100 separate docking calculations were performed. Each docking calculation consisted of 10 million energy evaluations using the Lamarckian genetic algorithm local search (GALS) method. The GALS method evaluates a population of possible docking solutions and propagates the most successful individuals from each generation into the subsequent generation of possible solutions. A low-frequency local search according to the method of Solis and Wets is applied to docking trials to ensure that the final solution represents a local minimum. All dockings described in this paper were performed with a population size of 250, and 300 rounds of Solis and Wets local search were applied with a probability of 0.06. A mutation rate of 0.02 and a crossover rate of 0.8 were used to generate new docking trials for subsequent generations, and the best individual from each generation was propagated over the next generation. The docking results from each of the 100 calculations were clustered on the basis of root-mean square deviation (rmsd; solutions differing by <2.0 Å) between the Cartesian coordinates of the atoms and were ranked on the basis of free energy of binding (ΔG_{AD4}). Because AD4 does not perform any structural optimization and EM of the complexes found, a molecular mechanics/energy minimization (MM/EM) approach was applied to refine the AD4 output. Refinement of the complexes was achieved by *in vacuo* EM with the Discover algorithm ($\varepsilon = 1$) using the steepest descent and conjugate gradient methods until a rmsd of 0.05 kcal/mol per Å was reached. Calculations converged toward a single solution in which the lowest-energy (ΔG_{AD4}) binding conformation also belonged to the most populated cluster ($f_{occ} = 85/100$). This conformation was chosen as starting point for subsequent 1 ns MD simulations (time step = 1 fs, $T = 300$ K) using the Discover algorithm (Accelrys) and the CVFF [63]. The backbone coordinates of the TM helices were fixed during the MD simulations because, without environmental constraints (i.e., lipid bilayer and water solution), they can move away from each other and can lose their helical structure. MD trajectory was analyzed by means of the analysis module of the InsightII package. Complex picture was rendered employing the UCSF Chimera software [65]. Rescoring of the ligand/receptor models according to the AD4 [64] scoring function was attained using a script provided within the MGLTools software package (http://mgltools.scripps.edu/).

The LC–MS and NMR spectral data were provided by Centro di Servizio Interdipartimentale di Analisi Strumentale (CSIAS), Università degli Studi di Napoli "Federico II". The assistance of the staff is gratefully appreciated. Part of this work was supported by Italian Ministry of Education, University and Research (PRIN 2008, 2008TSWB8K_002; PRIN 2009, 2009EL5WBP_004).

The authors have declared no conflict of interest.

References

[1] D. Pearson, J. E. Shively, B. R. Clark, I. I. Geschwind, M. Barkley, R. S. Nishioka, H. A. Bern, *Proc. Natl. Acad. Sci. USA* **1980**, *77*, 5021–5024.

[2] J. M. Conlon, F. O'Harte, D. D. Smith, M. C. Tonon, H. Vaudry, *Biochem. Biophys. Res. Commun.* **1992**, *188*, 578–583.

[3] J. C. Beauvillain, J. M. Conlon, H. A. Bern, H. Vaudry, *Proc. Natl. Acad. Sci. USA* **1998**, *95*, 15803–15808.

[4] Y. Coulouarn, S. Jegou, H. Tostivint, H. Vaudry, I. Lihrmann, *FEBS Lett.* **1999**, *457*, 28–32.

[5] M. Mori, T. Sugo, M. Abe, Y. Shimomura, M. Kurihara, C. Kitada, K. Kikuchi, Y. Shintani, T. Kurokawa, H. Onda, O. Nishimura, M. Fujino, *Biochem. Biophys. Res. Commun.* **1999**, *265*, 123–129.

[6] N. A. Elshourbagy, S. A. Douglas, U. Shabon, S. Harrison, G. Duddy, J. L. Sechler, Z. Ao, B. E. Maleef, D. Naselsky, J. Disa, N. V. Aiyar, *Br. J. Pharmacol.* **2002**, *136*, 9–22.

[7] R. S. Ames, H. M. Sarau, J. K. Chambers, R. N. Willette, R. V. Aiyar, A. M. Romanic, C. S. Louden, J. J. Foley, C. F. Sauermelch, R. W. Coatney, Z. Ao, J. Disa, S. D. Holmes, J. M. Stadel, J. D. Martin, W. S. Liu, G. I. Glover, S. Wilson, D. E. McNutty, C. E. Ellis, N. A. Eishourbagy, U. Shabon, J. J. Trill, D. V. P. Hay, E. H. Ohlstein, D. J. Bergsma, S. A. Douglas, *Nature* **1999**, *401*, 282–286.

[8] T. Sugo, Y. Murakami, Y. Shimomura, M. Harada, M. Abe, Y. Ishibashi, C. Kitada, N. Miyajima, N. Suzuki, M. Mori, M. Fujino, *Biochem. Biophys. Res. Commun.* **2003**, *310*, 860–868.

[9] D. Chatenet, C. Dubessy, J. Leprince, C. Boularan, L. Carlier, I. Segalas-Milazzo, L. Guilhaudis, H. Oulyadi, D. Davoust, E. Scalbert, B. Pfeiffer, P. Renard, M. C. Tonon, I. Lihrmann, P. Pacaud, H. Vaudry, *Peptides* **2004**, *25*, 1819–1830.

[10] N. Chartrel, J. M. Conlon, F. Collin, B. Braun, D. Waugh, M. Vallarino, S. L. Lahrichi, J. E. Rivier, H. Vaudry, *J. Comput. Neurol.* **1996**, *364*, 324–339.

[11] Y. Coulouarn, C. Fernex, S. Jegou, C. E. Henderson, H. Vaudry, I. Lihrmann, *Mech. Dev.* **2001**, *101*, 187–190.

[12] G. Pelletier, I. Lihrmann, H. Vaudry, *Neuroscience* **2002**, *115*, 525–532.

[13] G. Pelletier, I. Lihrmann, C. Dubessy, V. Luu-The, H. Vaudry, F. Labrie, *Neuroscience* **2005**, *132*, 689–696.

[14] E. Novellino, P. Grieco, M. Caraglia, A. Budillon, R. Franco, S. R. Addeo, *PCT Int. Appl.* **2008**, 21pp. WO 2008095995.

[15] J. J. Maguire, A. P. Davenport, *Br. J. Pharmacol.* **2002**, *137*, 579–588.

[16] S. A. Douglas, E. H. Ohlstein, *Trends Cardiovasc. Med.* **2000**, *10*, 229–237.

[17] S. A. Douglas, *Curr. Opin. Pharmacol.* **2003**, *3*, 159–167.

[18] R. A. Silvestre, E. M. Egido, R. Hernandez, J. Leprince, D. Chatenet, H. Tollemer, N. Chartrel, H. Vaudry, J. Marco, *Eur. J. Endocrinol.* **2004**, *151*, 803–809.

[19] T. Djordjevic, R. S. Belaiba, S. Bonello, J. Pfeilschifter, J. Hess, A. Gorlach, *Arterioscler. Thromb. Vasc. Biol.* **2005**, *25*, 519–525.

[20] Rd. Bianca, E. Mitidieri, F. Fusco, E. D'Aiuto, P. Grieco, E. Novellino, C. Imbimbo, V. Mirone, G. Cirino, R. Sorrentino, *PLoS ONE* **2012**, *7*, e31019.

[21] Y. Matsumoto, M. Abe, T. Watanabe, Y. Adachi, T. Yano, H. Takahashi, T. Sugo, M. Mori, C. Kitada, T. Kurokawa, M. Fujino, *Neurosci. Lett.* **2004**, *358*, 99–102.

[22] E. B. Maryanoff, A. W. Kinney, *J. Med. Chem.* **2010**, *53*, 2695–2708.

[23] P. Tsoukas, E. Kane, A. Giaid, *Front. Pharmacol.* **2011**, *2*, 1–11.

[24] E. Lescot, R. Bureau, S. Rault, *Peptides* **2007**, *29*, 680–690.

[25] V. J. Hruby, *Nat. Rev. Drug Discov.* **2002**, *1*, 847–858.

[26] H. Itoh, D. McMaster, K. Lederis, *Eur. J. Pharmacol.* **1988**, *149*, 61–66.

[27] S. Flohr, M. Kurz, E. Kostenis, A. Brkovich, A. Fournier, T. Klabunde, *J. Med. Chem.* **2002**, *45*, 1799–1805.

[28] W. A. Kinney, H. R. Almond, J. Qi, C. E. Smith, R. J. Santulli, L. de Garavilla, P. Andrade-Gordon, D. S. Cho, A. M. Everson, M. A. Feinstein, P. A. Leung, B. E. Maryanoff, *Angew. Chem. Int. Ed.* **2002**, *41*, 2940–2944.

[29] A. Brkovic, A. Hattenberger, E. Kostenis, T. Klabunde, S. Flohr, M. Kurz, S. Bourgault, *J. Pharmacol. Exp. Ther.* **2003**, *306*, 1200–1209.

[30] P. Labarrere, D. Chatenet, J. Leprince, C. Marionneau, G. Loirand, M. C. Tonon, C. Dubessy, E. Scalbert, B. Pfeiffer, P. Renard, B. Calas, P. Pacaud, H. Vaudry, *J. Enzyme Inhib. Med. Chem.* **2003**, *18*, 77–88.

[31] D. H. Coy, W. J. Rossowski, B. L. Cheng, J. E. Taylor, *Peptides* **2002**, *23*, 2259–2264.

[32] A. Carotenuto, P. Grieco, E. Novellino, P. Rovero, *Med. Res. Rev.* **2004**, *24*, 577–588.

[33] A. Carotenuto, P. Grieco, P. Rovero, E. Novellino, *Curr. Med. Chem.* **2006**, *13*, 267–275.

[34] P. Grieco, A. Carotenuto, R. Patacchini, C. A. Maggi, E. Novellino, P. Rovero, *Bioorg. and Med. Chem.* **2002**, *10*, 3731–3739.

[35] P. Grieco, A. Carotenuto, P. Campiglia, E. Zampelli, R. Patacchini, C. A. Maggi, E. Novellino, P. Rovero, *J. Med. Chem.* **2002**, *45*, 4391–4394.

[36] R. Patacchini, P. Santicioli, S. Giuliani, P. Grieco, E. Novellino, P. Rovero, C. A. Maggi, *Br. J. Pharmacol.* **2003**, *140*, 1155–1158.

[37] V. Camarda, W. Song, E. Marzola, M. Spagnol, R. Guerrini, S. Salvadori, D. Regoli, J. P. Thompson, D. J. Rowbotham, D. J. Behm, S. A. Douglas, G. Calò, D. G. Lambert, *Eur. J. Pharmacol.* **2004**, *498*, 83–86.

[38] J. Zhao, Q. X. Yu, W. Kong, H. C. Gao, B. Sun, Y. Q. Xie, L. Q. Ren, *Exp. Ther. Med.* **2013**, *6*, 1765–1769.

[39] A. Carotenuto, P. Grieco, P. Campiglia, E. Novellino, P. Rovero, *J. Med. Chem.* **2004**, *47*, 1652–1661.

[40] P. Grieco, A. Carotenuto, P. Campiglia, L. Marinelli, T. Lama, R. Patacchini, P. Santicioli, C. A. Maggi, P. Rovero, E. Novellino, *J. Med. Chem.* **2005**, *48*, 7290–7297.

[41] P. Grieco, A. Carotenuto, P. Campiglia, I. Gomez-Monterrey, L. Auriemma, M. Sala, C. Marcozzi, R. d'Emmanuele di Villa Bianca, D. Brancaccio, P. Rovero, P. Santicioli, S. Meini, C. A. Maggi, E. Novellino, *J. Med. Chem.* **2009**, *52*, 3927–3940.

[42] A. Carotenuto, L. Auriemma, F. Merlino, A. Limatola, P. Campiglia, I. Gomez-Monterrey, R. d'Emmanuele di Villa Bianca, D. Brancaccio, P. Santicioli, S. Meini, C. A. Maggi, E. Novellino, P. Grieco, *J. Pept. Sci.* **2013**, *19*, 293–300.

[43] K. Wüthrich, *NMR of Proteins and Nucleic Acids*, John Wiley & Sons, Inc., New York **1986**.

[44] U. Piantini, O. W. Sorensen, R. R. Ernst, *J. Am. Chem. Soc.* **1982**, *104*, 6800–6801.

[45] D. Marion, K. Wüthrich, *Biochem. Biophys. Res. Commun.* **1983**, *113*, 967–974.

[46] L. Braunschweiler, R. R. Ernst, *J. Magn. Reson.* **1983**, *53*, 521–528.

[47] J. Jenner, B. H. Meyer, P. Bachman, R. R. Ernst, *J. Chem. Phys.* **1979**, *71*, 4546–4553.

[48] C. Bartels, T. Xia, M. Billeter, P. Güntert, K. Wüthrich, *J. Biomol. NMR* **1995**, *6*, 1–10.

[49] K. Palczewski, T. Kumasaka, T. Hori, C. A. Behnke, H. Motoshima, B. A. Fox, I. Le Trong, D. C. Teller, T. Okada, T. E. Stenkamp, M. Yamamoto, M. Miyano, *Science* **2000**, *289*, 739–745.

[50] V. Cherezov, D. M. Rosenbaum, M. A. Hanson, S. G. Rasmussen, F. S. Thian, T. S. Kobilka, H. J. Choi, P. Kuhn, W. I. Weis, B. K. Kobilka, R. C. Stevens, *Science* **2007**, *318*, 1258–1265.

[51] C. Haskell-Luevano, K. Toth, L. Boteju, C. Job, A. M. Castrucci, M. E. Hadley, V. J. Hruby, *J. Med. Chem.* **1997**, *40*, 2740–2749.

[52] P. Grieco, L. Giusti, A. Carotenuto, P. Campiglia, V. Calderone, T. Lama, I. Gomez-Monterrey, G. Tartaro, M. R. Mazzoni, E. Novellino, *J. Med. Chem.* **2005**, *48*, 3153–3163.

[53] D. D'Addona, A. Carotenuto, E. Novellino, V. Piccand, J. C. Reubi, A. Di Cianni, F. Gori, A. M. Papini, M. Ginanneschi, *J. Med. Chem.* **2008**, *51*, 512–520.

[54] A. Di Cianni, A. Carotenuto, D. Brancaccio, E. Novellino, J. C. Reubi, K. Beetschen, A. M. Papini, M. Ginanneschi, *J. Med. Chem.* **2010**, *53*, 6188–6197.

[55] T. Yamamoto, P. Nair, T. M. Largent-Milnes, N. E. Jacobsen, P. Davis, S. W. Ma, H. I. Yamamura, T. W. Vanderah, F. Porreca, J. Lai, V. J. Hruby, *J. Med. Chem.* **2011**, *54*, 2029–2038.

[56] P. Grieco, D. Brancaccio, E. Novellino, V. J. Hruby, A. Carotenuto, *Eur. J. Med. Chem.* **2011**, *46*, 3721–3733.

[57] M. R. Saviello, S. Malfi, P. Campiglia, A. Cavalli, P. Grieco, E. Novellino, A. Carotenuto, *Biochemistry* **2010**, *49*, 1477–1485.

[58] P. Grieco, A. Carotenuto, L. Auriemma, M. R. Saviello, P. Campiglia, I. Gomez-Monterrey, L. Marcellini, V. Luca, D. Barra, E. Novellino, M. L. Mangoni, *Biochim. Biophys. Acta* **2013**, *1828*, 652–660.

[59] T. L. Hwang, A. J. Shaka, *J. Magn. Res.* **1995**, *112*, 275–279.

[60] D. J. States, R. A. Haberkorn, D. J. Ruben, *J. Magn. Reson.* **1982**, *48*, 286–292.

[61] P. Güntert, C. Mumenthaler, K. Wüthrich, *J. Mol. Biol.* **1997**, *273*, 283–298.

[62] R. Koradi, M. Billeter, K. Wüthrich, *J. Mol. Graph.* **1996**, *14*, 51–55.

[63] J. Maple, U. Dinur, A. T. Hagler, *Proc. Natl. Acad. Sci. USA* **1988**, *85*, 5350–5353.

[64] R. Huey, G. M. Morris, A. J. Olson, D. S. Goodsell, *J. Comput. Chem.* **2007**, *28*, 1145–1152.

[65] E. F. Pettersen, T. D. Goddard, C. C. Huang, G. S. Couch, D. M. Greenblatt, E. C. Meng, T. E. Ferrin, *J. Comput. Chem.* **2004**, *25*, 1605–1612.

